



Modeling of quasi-grating sidewall corrugation in SOI microring add-drop filters

Tao Wang^a, Ziyang Zhang^b, Fangfei Liu^a, Ye Tong^a, Jing Wang^b, Yue Tian^a, Min Qiu^b, Yikai Su^{a,*}

^aState Key Lab of Advanced Optical Communication Systems and Networks, Shanghai Jiao Tong University, Shanghai 200240, China

^bDepartment of Microelectronics and Applied Physics, Royal Institute of Technology, Electrum 229, 164 40 Kista, Sweden

ARTICLE INFO

Article history:

Received 15 March 2009

Received in revised form 26 May 2009

Accepted 26 May 2009

Keywords:

Integrated optics

Resonators

Sidewall corrugation

Quasi-grating

ABSTRACT

We build a model to study the sidewall corrugation of fabricated silicon microrings and investigate its impact on the spectral response of the resonator system. From the scanning electron microscope images, the sidewall corrugation can be engineered into certain periodicity and characterized into a group of rectangular gratings, or quasi-gratings, which in turn generate mutual mode coupling between the forward- and backward-propagating modes in the ring and lead to resonance splitting. We find that the reflectivity of the quasi-gratings is proportional to the mutual coupling strength and the resonance splitting only occurs at the resonances where high reflectivity takes place. The model agrees well with the experimental measurements and provides some guideline in applying mutual mode coupling for various functions in the field of optics.

© 2009 Elsevier B.V. All rights reserved.

1. Introduction

Devices based on silicon microrings have found applications in many areas, including optical filtering/add-drop multiplexing [1], signal processing [2–4], bio-sensing [5], etc. High-quality-factor microrings of various materials are often desired and some studies [6–8] have been carried out to deal with the surface corrugation, which leads to propagation loss in the dielectric waveguides [9,10]. It is also found that apart from inducing scattering losses, the sidewall corrugation can induce back-reflection and may generate the counter-propagating mode in the ring. The mutual coupling between the forward and backward modes can lead to the splitting of resonance peaks [11]. At the first glance, this might not be desirable in some applications, such as filtering and modulating. However, if further explored, sidewall corrugation can be designed and engineered [12], and the resulting resonance splitting can be utilised for many important functions, such as fast light in over-coupled region [13], continuously-tunable slow- to fast light in double-waveguide coupled resonators [14], dense wavelength conversion and multicasting [15], format conversion from non-return-to-zero (NRZ) to frequency-shift-keying (FSK) [16], and optical up-conversion in radio over fibre (RoF) systems [17]. Thus, it becomes necessary to analyze the characteristics of the sidewall corrugation and build a model for designing the desired gratings under different conditions.

In this paper, we investigate the characteristics of the sidewall corrugation structure as well as its impact on the spectral response

of microring resonators. Unlike the random perturbation evaluation based on antenna theory [18], we estimate the corrugation analogous to a structure comprising of gratings with rectangular shape. Furthermore, the transmission response of microring resonators is evaluated in the presence of the grating reflectivity, which is considered as a lumped reflection coefficient. It turns out that resonance splitting, including the occurrence, location and degree, is determined by the distribution of the sidewall quasi-gratings in our model. The spectral responses for different resonators obtained from the model are in good agreement with the experimental measurements. Thus, split resonances can be deliberately generated and eliminated by engineering the sidewall gratings to satisfy a variety of practical applications.

2. Structure of the quasi-grating corrugation

In previous works [18], the sidewall corrugation was considered as random perturbations with variable depths and the reflectivity induced by the corrugation was interpreted as a stochastic average. However, the scanning electron microscope (SEM) photos of our device, shown in Fig. 1, tell another story. The corrugation resembles a group of ridges, which appear to have similar amplitude and period. This traces back to the fabrication process. During the electron beam lithography (Raith 150, 25 kV) a circular exposure line is actually broken down into a closed polygene path, forming edges and corners in the microring structure. Along each edge, there are a limited number of actual exposure dots with the same step size. Together with the limited material resolution of the negative resist (maN2405), some 30–50 nm ridges are formed in a semi-periodic manner along the microring sidewalls. Based on the SEM

* Corresponding author. Tel.: +86 021 34204356; fax: +86 021 34204370.
E-mail address: yikaisu@sjtu.edu.cn (Y. Su).

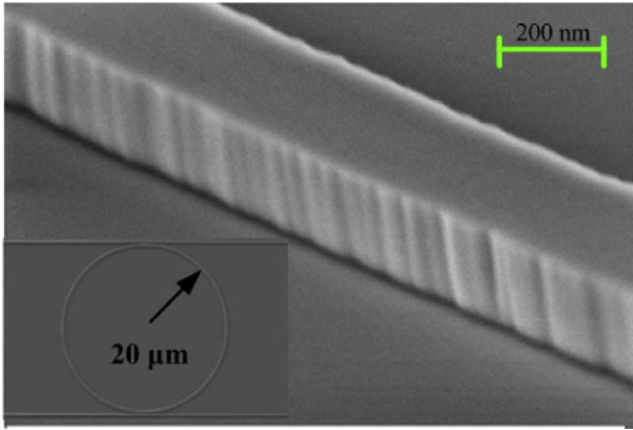


Fig. 1. The SEM photograph of the quasi-gratings along the sidewall of the microring resonator. Inset is the corresponding microring resonator with a radius of $\sim 20 \mu\text{m}$.

photos and the understanding of the fabrication process, we treat the sidewall corrugation analogous to several rectangular gratings with the same size and period, only separated with different distances, as depicted in Fig. 2. The zoom-in view in the left shows the detailed structure for one of the gratings with its period and length being denoted as Λ and L , respectively. Due to the SEM limitation, the exact structure of the quasi-grating sidewall roughness is difficult to observe. Therefore, we only empirically estimate the distance between the groups of ridges, which is not included in the equations for model fitting.

3. Reflectivity of the gratings

We illustrate the effective reflection of the quasi-gratings based on the conventional principle for gratings. To simplify the analysis, we only consider the first-order diffraction condition. For a single grating, the reflectivity r can be expressed as [19],

$$r = \begin{cases} \frac{\kappa^2 \sinh^2(SL)}{\delta^2 \sinh^2(SL) + S^2 \cosh^2(SL)} & \text{for } \kappa > \delta \\ \frac{\kappa^2 \sin^2(QL)}{\delta^2 \sin^2(QL) + Q^2 \cos^2(QL)} & \text{for } \kappa < \delta \end{cases} \quad (1)$$

where $S = \sqrt{\kappa^2 - \delta^2}$ and $Q = \sqrt{\delta^2 - \kappa^2}$ are satisfied. Here, $\delta = 2\pi n_{\text{eff}}/\lambda - \pi/\Lambda$ is the detuned propagation constant and κ is the coupling coefficient of the grating for TE-mode, which is similar to [20]:

$$\kappa = \frac{\pi(n_{\text{co}}^2 - n_{\text{cl}}^2)}{n_{\text{eff}}} \sin\left(\frac{\pi d}{\Lambda}\right) (1 - \Gamma) \frac{1}{\lambda} \quad (2)$$

where $n_{\text{eff}} = 2.6$ is the effective refractive index for the fundamental mode and $n_{\text{co}}^2 - n_{\text{cl}}^2$ is the core (Si)-cladding (SiO_2) relative permittivity contrast. As shown in Fig. 2, the ridge width is d and we assume that the duty cycle [21] of the grating (d/Λ) is 50%. Since only a fraction of energy unconfined in the waveguide core is affected by the corrugation, the coefficient $(1 - \Gamma)$ is involved in estimating the value of κ . We choose the confinement factor $\Gamma = 0.9$, which is typical for Si/ SiO_2 single mode waveguide [22]. Thus, $\kappa \approx 1/\lambda$ is obtained.

Specifically, we explore the quasi-grating corrugation along a microring resonator with the radius of $\sim 20 \mu\text{m}$. Since the pseudo-circular scan mode in E-beam generates nodes with period around one hundred nanometers [11] and generally signal processing is carried out in C band, we evaluate the reflectivity of the quasi-gratings in the wavelength from 1540 to 1560 nm with the grating period around 100 nm. As a result, the Bragg wavelength is $\sim 500 \text{ nm}$ based on the diffraction theory ($\lambda_{\text{Bragg}} = 2n\Lambda$, $n \approx 2.5$). The impact of high order harmonics of the rectangular grating is negligible as they correspond to shorter wavelengths. Since the interested wavelength range is far away from the Bragg wavelength, the reflectivity of a single grating is very small ($r \ll 1$). Thus, the overall effective reflectivity of the quasi-gratings R is simply expressed as:

$$R = 1 - (1 - r)^N \quad (3)$$

where N is total number of the gratings along the ring. We consider the reflectivity variation of the corrugation with different grating features. Firstly, we assume that the corrugation composes of four gratings ($N = 4$) with the same length of $25 \mu\text{m}$ as the circumference of the ring is $\sim 125 \mu\text{m}$ and there is a distance between every two adjacent gratings. Based on the analysis above, we plot the reflectivity variations as a function of the wavelength with grating periods of 80, 100, and 120 nm, respectively.

Fig. 3 shows that both the average value and variation range of the reflectivity increases with the grating period lengthening. Furthermore, we fix the grating period at 100 nm and study the reflection feature with various grating distributions. Besides the one already analyzed (four gratings with the same length of $25 \mu\text{m}$), we evaluate another two structures for comparison. One is formed by seven gratings ($N = 7$) with the same length of $16 \mu\text{m}$ and the other one comprises two gratings ($N = 2$) with the same length of $45 \mu\text{m}$. Fig. 4 displays their different characteristics. In the interested wavelength range, the reflectivity experiences two “peak to valley” courses for the structure with grating length of $45 \mu\text{m}$, while it experiences only once for the other two structures. Thus, the grating length should be shortened if a slowly varied reflectivity is desired. Moreover, the average reflectivity decreases with the increasing of grating length.

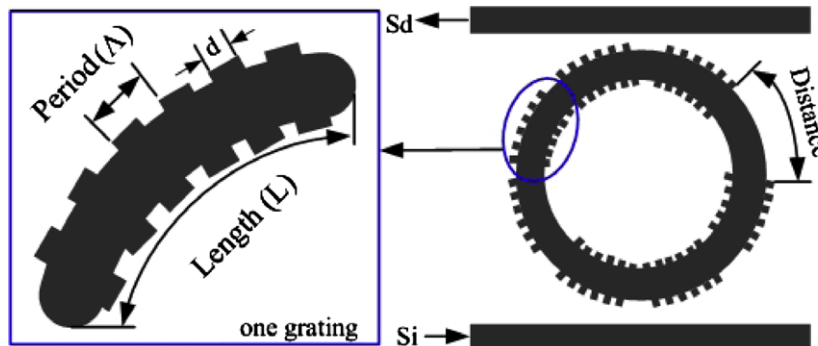


Fig. 2. Schematic of microring resonator with sidewall corrugation analogous to rectangular gratings.

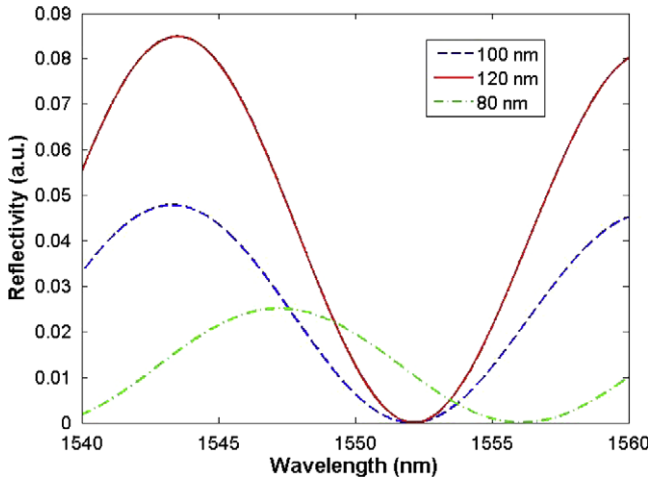


Fig. 3. Reflectivity variation as a function of the wavelength with different grating periods.

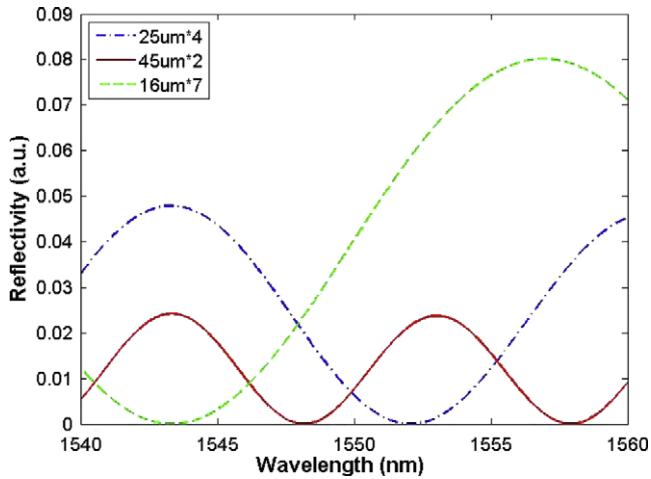


Fig. 4. Reflectivity variation as a function of the wavelength with different grating lengths.

4. Spectral responses of the resonators with sidewall gratings

To verify the reliability of our model and investigate its influence on the spectral responses, we discuss three different microring resonators. The inset of Fig. 1 shows one of the resonators, which are fabricated on a commercial single-crystalline SOI wafer with a 250-nm-thick silicon slab on top of a 3- μm silica cladding layer. The cross section of the silicon waveguide is $450 \times 250 \text{ nm}^2$ with an effective area of $0.1 \mu\text{m}^2$ for the transverse-electric (TE) mode. The microring is sandwiched between two straight waveguides with an air gap of 120 nm. The measured spectral responses (blue solid curves) through the drop channels of the three resonators are shown in Fig. 5a, d, and g, respectively.

It can be seen that their characteristics are quite different from each other and the resonance splitting only occurs at certain wavelengths in every resonator. Considering the quasi-gratings' effective reflectivity R as a lumped reflection coefficient conforming to the characteristics of the built model and using steady-state loop equations [18], we evaluate the corresponding spectral response as:

$$\frac{S_d}{S_i} = -j \frac{\kappa_1^2}{1 - t_k^2 A \exp(-j4\pi^2 R_0 n_g / \lambda)} \quad (4)$$

$$A = \frac{\sqrt{1 - R} - t_k^2 \exp(-j4\pi^2 R_0 n_g / \lambda)}{1 - \sqrt{1 - R} t_k^2 \exp(-j4\pi^2 R_0 n_g / \lambda)} \quad (5)$$

where R_0 is the ring radius around $20 \mu\text{m}$ and the group index $n_g = 4.1$ is estimated from the measured free spectral range (FSR) of the resonators. $t_k = \sqrt{1 - \kappa_1^2}$ is the transmission coefficient associated with the coupling coefficient κ_1 between the ring and one adjacent waveguide. $\kappa_1 = 0.17$ is derived based on the resonance spectrum measurements and calculations as [23]. Using Eqs. (4) and (5), the fitted transmission responses (red dashed curves) for all of the three resonators are depicted. The resonance splitting degree and distribution are proved to be determined by the reflection characteristics of the quasi-gratings in the spectral fitting.

For the resonator with the spectral response shown in Fig. 5a, we find that the phenomenon of peak splitting takes place at only one resonance and the peak values of the resonances are different. Once a resonance wavelength matches a high reflectivity, the peak splitting appears. Since the reflectivity feature can be modified by adjusting the number of gratings (N) and the length (L) of one grating, a preliminary spectral fitting is achieved with the corrugation structure consisting of four gratings with the same length of $25 \mu\text{m}$. In addition, a little variation of the ring radius and grating period will also influence the resonances and reflection features, respectively. As a result, the spectrum fits to the measured one more accurately when the grating period and ring radius are set as 109.82 nm and $19.99 \mu\text{m}$, respectively. Fig. 5b and c displays two zoom-in resonance peaks and it can be seen that the simulated resonances based on our built model agrees well with the measured results. Similarly, the other two measured transmission responses can also be fitted based on our model. Fig. 5d shows the spectra of another resonator. Peak splitting appears in three consecutive resonances, implying that the reflectivity varies slowly and all of the three resonances correspond to a high reflectivity, which can be achieved by decreasing the grating length ($L = 16 \mu\text{m}$) in accompany with the grating number increasing ($N = 7$) according to the analysis above. Besides, the optimal grating period is 108.93 nm and the ring radius goes up to $20.39 \mu\text{m}$ since the free spectral range becomes narrower. Fig. 5e and f shows two detailed split resonances around 1549.4 and 1554 nm , respectively. A minor reflectivity difference induces the discrepancy of their splitting degree. From the spectra illustrated in Fig. 5g for the third resonator, it is obvious that a fast reflectivity variation takes place leading to a modification of the corrugation structure, which is composed of two gratings ($N = 2$) with the same length of $\sim 45 \mu\text{m}$. The optimal grating period is 109.28 nm and the ring radius slightly changes to $20.4 \mu\text{m}$. It can be seen from the zoom-in resonances in Fig. 5h and i that no splitting occurs due to the relatively low average reflectivity of the quasi-gratings, as depicted in Fig. 3b. There is some discrepancy between the fitted spectra and measured ones due to the imperfections of measurement instruments and the noise floors.

5. Conclusion

We investigate and build a model for the quasi-grating corrugation along the sidewall of microring resonators. Since the corrugation consists of rectangular quasi-gratings according to the SEM photographs, its reflectivity can be estimated using the conventional theory. Also, the impact of the corrugation on the spectral response of resonators is studied. From the measured three transmission spectra and the corresponding fitted ones, it is found that the occurrence of the split resonances and their splitting degree are affected by the quasi-gratings' reflection feature, which

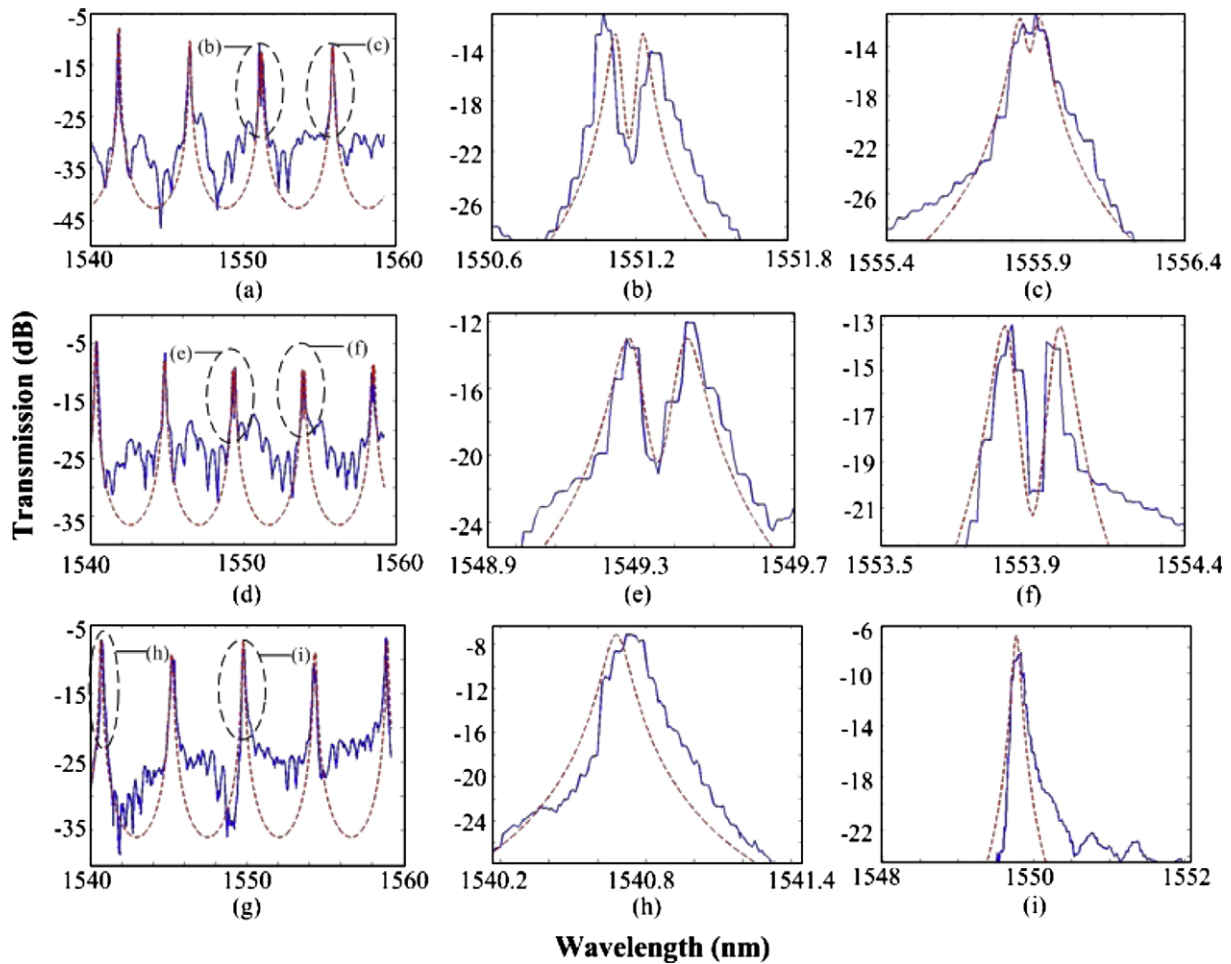


Fig. 5. Transmission spectra (a), (d), and (g) and the corresponding zoom-in resonances (b, c), (e, f), and (h, i) for the resonators with different sidewall corrugation structures.

is determined by the grating period and length. Thus, it sheds some insights on the design of the grating-assisted microrings when the grating period and length can be controlled precisely in the fabrication systems.

Acknowledgement

The authors acknowledge the support from the National Natural Science Foundation of China (60777040), and the Shanghai Rising Star Program Phase II (07QH14008), the Swedish Foundation for Strategic Research (SSF), the Swedish Research Council (VR).

References

- [1] F. Xia, M. Rooks, L. Sekaric, Y. Vlasov, *Opt. Express* 15 (2007) 11934.
- [2] Q. Xu, V.R. Almeida, M. Lipson, *Opt. Lett.* 20 (2005) 2733.
- [3] F. Xia, L. Sekaric, Y. Vlasov, *Nat. Photon.* 1 (2007) 65.
- [4] B. Lee, B. Small, K. Bergman, Q. Xu, M. Lipson, *Opt. Lett.* 31 (2006) 2701.
- [5] K. De Vos, I. Bartolozzi, E. Schacht, P. Bienstman, R. Baets, *Opt. Express* 15 (2007) 7610.
- [6] D. Rafizadeh, J.P. Zhang, R.C. Tiberio, S.T. Ho, *J. Lightwave Technol.* 16 (1998) 1308.
- [7] C.Y. Chao, L.J. Guo, *Appl. Phys. Lett.* 84 (2004) 2479.
- [8] V. Van, P.P. Absil, J.V. Hryniewicz, P.-T. Ho, *J. Lightwave Technol.* 19 (2001) 1734.
- [9] C.G. Poulton et al., *IEEE J. Sel. Top. Quantum Electron.* 12 (2006) 1306.
- [10] D. Marcuse, *Bell Syst. Tech. J.* 48 (1969) 3187.
- [11] Z. Zhang, M. Dainese, L. Wosinski, M. Qiu, *Opt. Express* 16 (2008) 4621.
- [12] Q. Li, Z. Zhang, J. Wang, M. Qiu, Y. Su, *Opt. Express* 17 (2009) 933.
- [13] T. Wang, F. Liu, T. Ye, Z. Zhang, J. Wang, Y. Tian, M. Qiu, Y. Su, in: *Proceedings of Optical Fiber Communication (OFC), Paper OWC4*, 2009.
- [14] Z. Zhang, Q. Li, F. Liu, T. Ye, Y. Su, M. Qiu, in: *Proceedings of CLEO/QELS, Paper CTuT2*, 2008.
- [15] Q. Li, Z. Zhang, F. Liu, M. Qiu, Y. Su, *Appl. Phys. Lett.* 93 (2008) 081113.
- [16] F. Liu, Q. Li, Z. Zhang, M. Qiu, Y. Su, *Proc. SPIE* 7135 (2008) 713537.
- [17] Q. Chang, Q. Li, Z. Zhang, M. Qiu, Y. Su, in: *Proceedings of Optical Fiber Communication (OFC), Paper JWA48*, 2009.
- [18] B.E. Little, S.T. Chu, *Opt. Lett.* 22 (1997) 4.
- [19] C.R. Giles, *J. Lightwave Technol.* 15 (1997) 1391.
- [20] W. Streifer, D.R. Scifres, R.D. Burnham, *IEEE J. Quantum Electron.* 11 (1975) 867.
- [21] D. Wiesmann, R. Germann, G. Bona, *J. Opt. Soc. Am. B* 20 (2003) 417.
- [22] C. Manolatou, M. Lipson, *J. Lightwave Technol.* 24 (2006) 433.
- [23] F. Liu, Q. Li, Z. Zhang, M. Qiu, Y. Su, *IEEE J. Sel. Top. Quantum Electron.* 14 (2008) 706.